Supplement of Nat. Hazards Earth Syst. Sci., 24, 1341–1355, 2024
https://doi.org/10.5194/nhess-24-1341-2024-supplement


Natural Hazards and Earth System Sciences
Open Access
EGU

*Supplement of*

# Assessment of wind–damage relations for Norway using 36 years of daily insurance data

**Ashbin Jaison et al.**

*Correspondence to:* Ashbin Jaison (ashbin.jaison@uib.no)

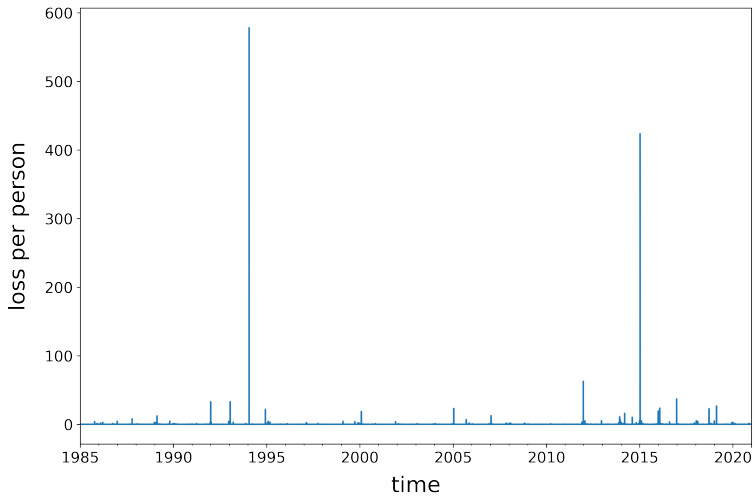


Figure S1: Example of time series of daily insurance loss per person (in NOK, 2015 values) for an arbitrary municipality.

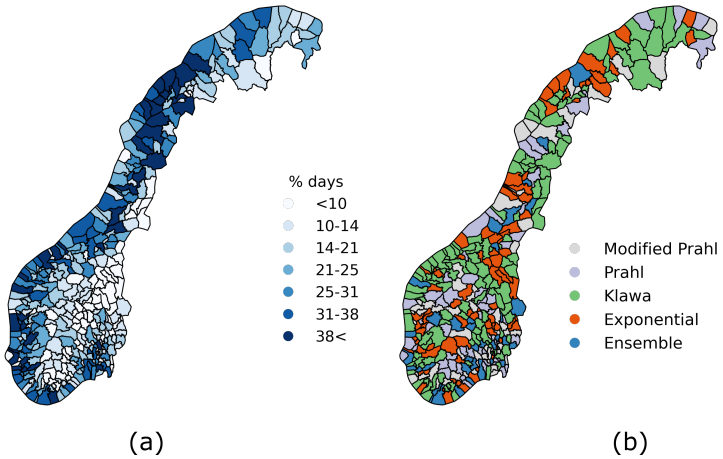


Figure S2: (a) Map showing the proportion of non-zero loss days above the 98th percentile wind speed in all Norwegian municipalities, (b) map indicating which models show the smallest MAE.

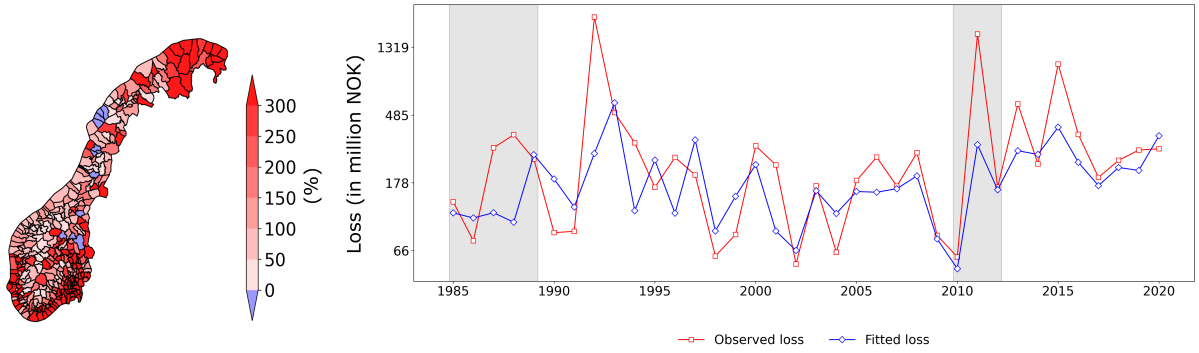


(a) (b)

Figure S3: (a) Relative difference in the smallest MAE of storm damage functions fitted at municipality and national level, (b) annually-aggregated national losses using all the loss days from the insurance data (red line) along with the annual national loss estimates (blue line), which are the sum of each municipality's best-performing-model estimate. Note that the y-axis is logarithmic, and the shaded region represents the testing period.

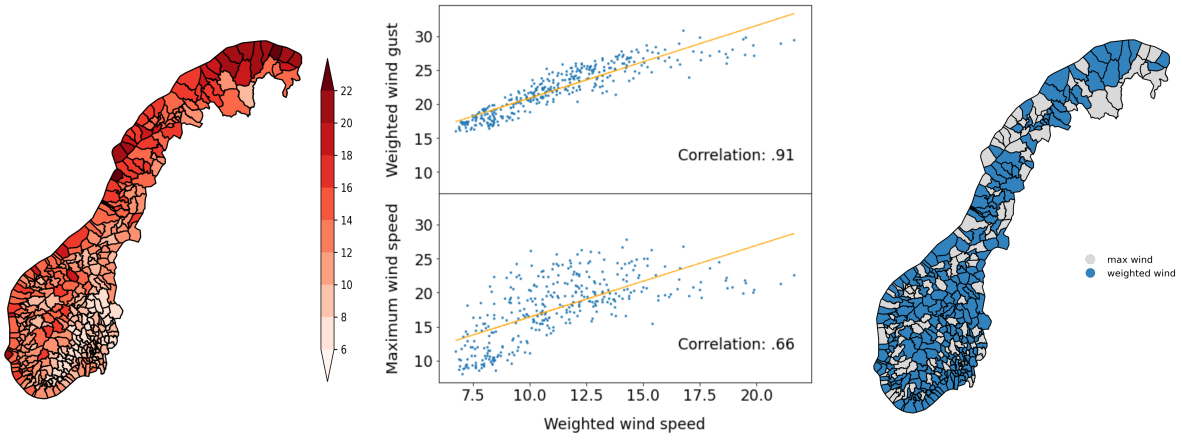


(a) (b) (c)

Figure S4: (a) Map showing the 98th percentile of the population-weighted daily maximum wind speed for each municipality for the period 1985-2020. (b) Spatial correlations between the 98th percentile of the population-weighted daily maximum wind speed and the 98th percentile of the population-weighted daily wind gust (top) and the 98th percentile of the daily maximum wind speed (bottom) and (c) municipalities with smallest CV among the five models with weighted and maximum wind speeds on test data. Municipalities in grey (blue) are where maximum (weighted) wind speed shows the lowest CV.

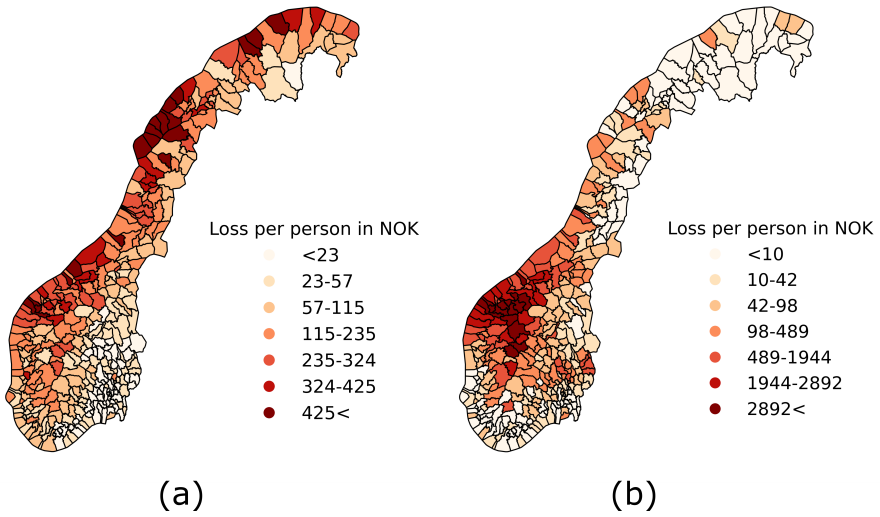


Figure S5: Maps of Norway showing (a) the annual average loss per person in each municipality during the study period 1985-2020 and (b) the average loss per person in each municipality caused by the storm Dagmar (25.12.2011-27.12.2011). To account for the skewness involved in the loss data and for meaningful visualization, the loss is split non-linearly with class boundaries at the 20th, 40th, 60th, 80th, 90th and 95th percentiles.

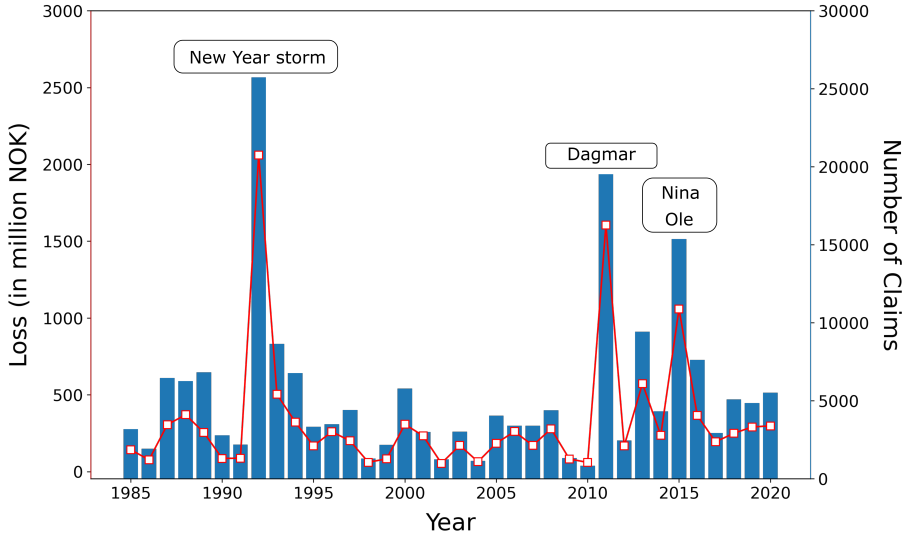


Figure S6: Annual number of insurance claims (blue bars) and monetary losses (red line, 2015 inflation-adjusted) associated with strong wind events in Norway from 1985 to 2020.

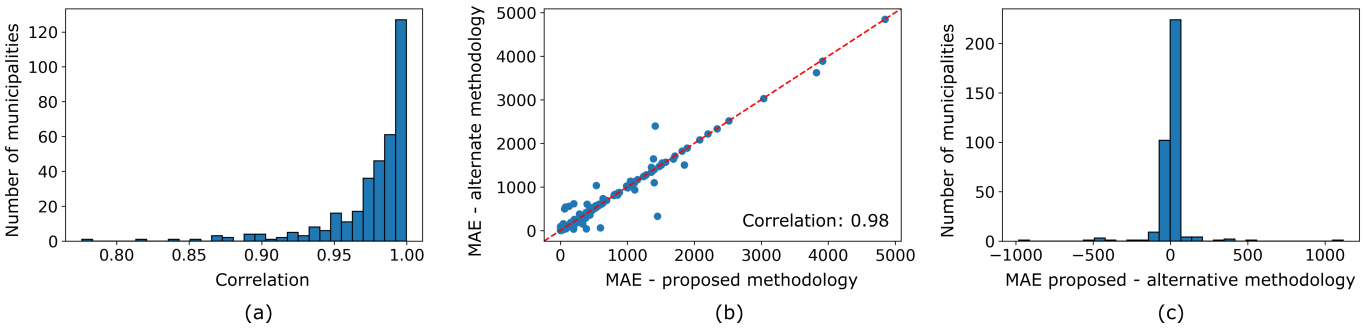


Figure S7: (a) Distribution of the Pearson correlation coefficient between the damage functions using the proposed (ours) and the alternate methodologies, (b) scatter plot of the MAEs of the extreme loss (losses above the 99.7th percentile) estimates for the proposed and the alternate methodologies using the testing data. Blue dots represent individual municipalities and the dashed red line represents the 1:1 line. (c) Distribution of MAE differences between the proposed and the alternate methodologies.

In our study, we weight the wind speed with population first and then aggregate it to the municipality resolution before calculating the loss index (Klawa's damage function, $d(\nu)$ from eq. 2). However, previous studies, such as Pinto et al. (2007), just weighted the resulting loss index. We here compare the two methodologies. We find a high correlation between both damage functions (Fig. S7a). Upon calibrating the two damage functions with municipality level insurance losses using eq. 3, we observe that in the extreme loss class MAEs are highly correlated with each other (Fig. S7b). Moreover, we find that their magnitudes are similar, with about 91.6% of the municipalities having MAE differences within [-70, 70] NOK/person in the testing data (Fig. S7c). However, when not distinguishing loss classes, we find that the alternative method (such as in Pinto et al., 2007) has better skill in estimating the losses, although this result depends on the model evaluation metric used (not shown). Thus, there is no conclusive evidence for one of the methods exhibiting a higher predictive skill than the other.

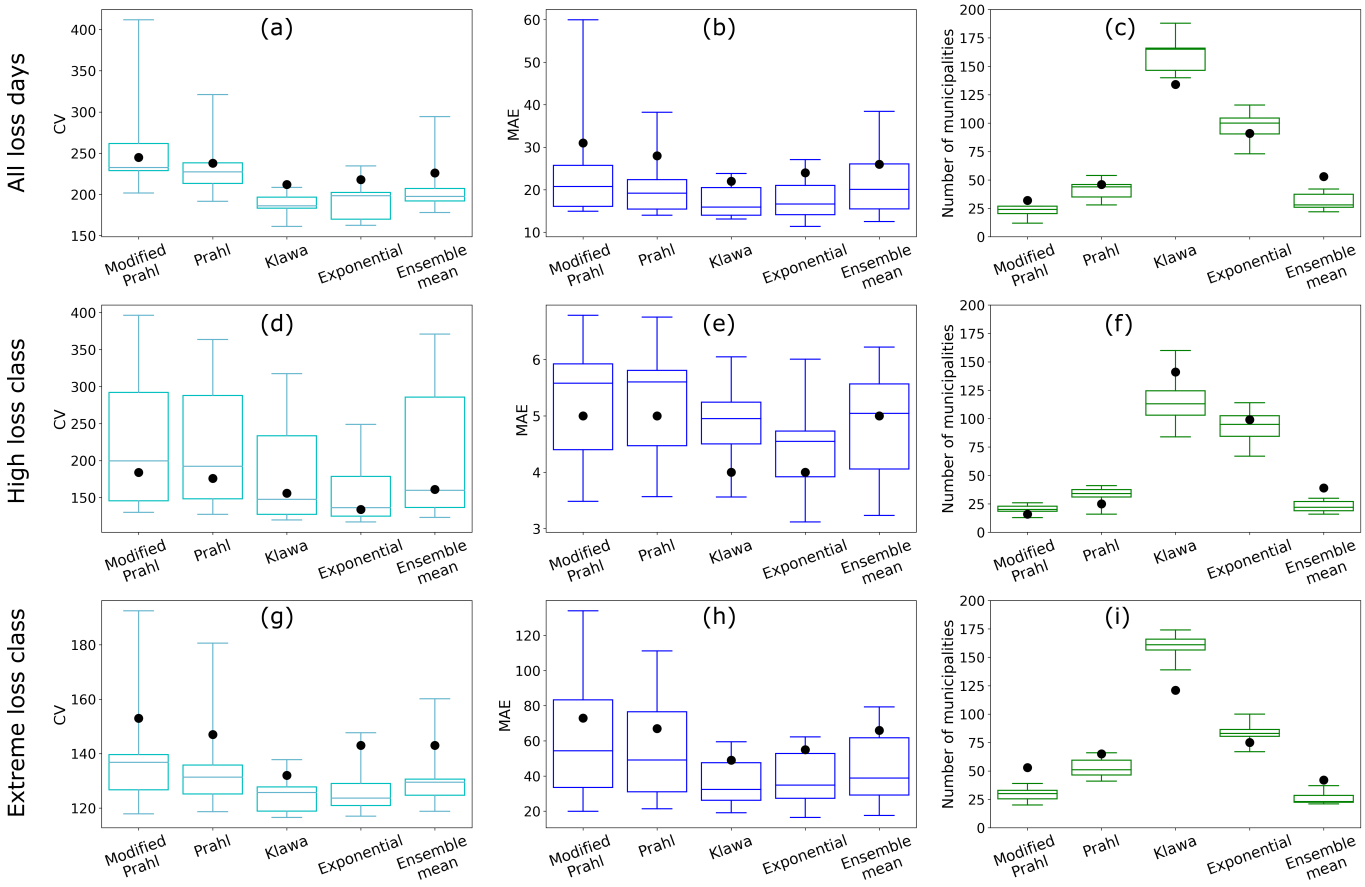


Figure S8: Distribution of model performance metrics from cross-validation (a) coefficient of variance (CV), (b) mean absolute error (MAE), (c) number of municipalities with smallest MAE for four damage functions and their ensemble mean for all loss days. (d), (e) and (f) same as (a), (b) and (c) but for the high loss class. (g), (h) and (i) same as (a), (b) and (c) but for the extreme loss class. The boxes represent the interquartile range, the horizontal line represents the median, the whiskers represent the minimum and maximum and the black dots represent the results from Table 1 in the manuscript.

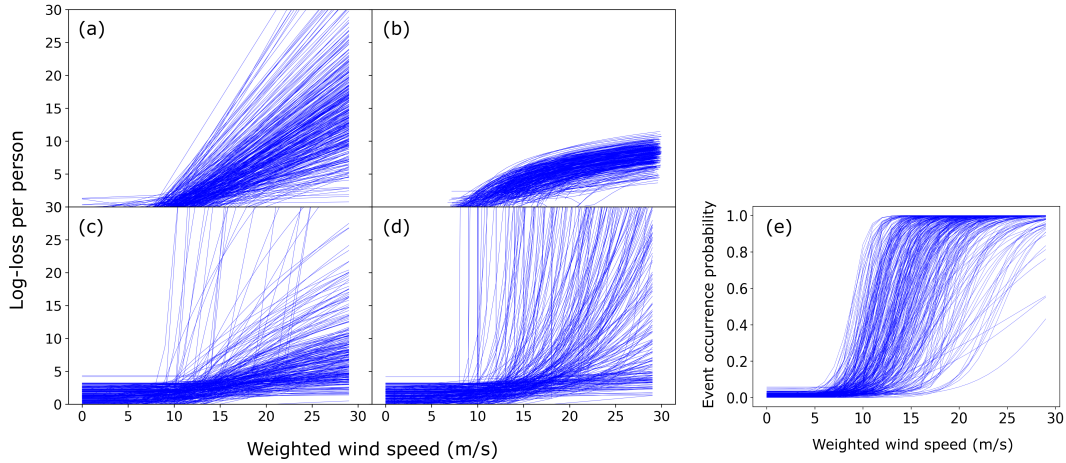


Figure S9: Shapes of the damage functions for all municipalities for (a) the exponential damage function, (b) the cubic excess over threshold damage function, (c) the magnitude term in the probabilistic damage function by Prahl, and (d) the magnitude term in the modified Prahl probabilistic damage function, (e) sigmoid function that estimates the probability of an event occurrence. Note that the y-axis for (a)-(d) represents the log-loss per person with units of log NOK.

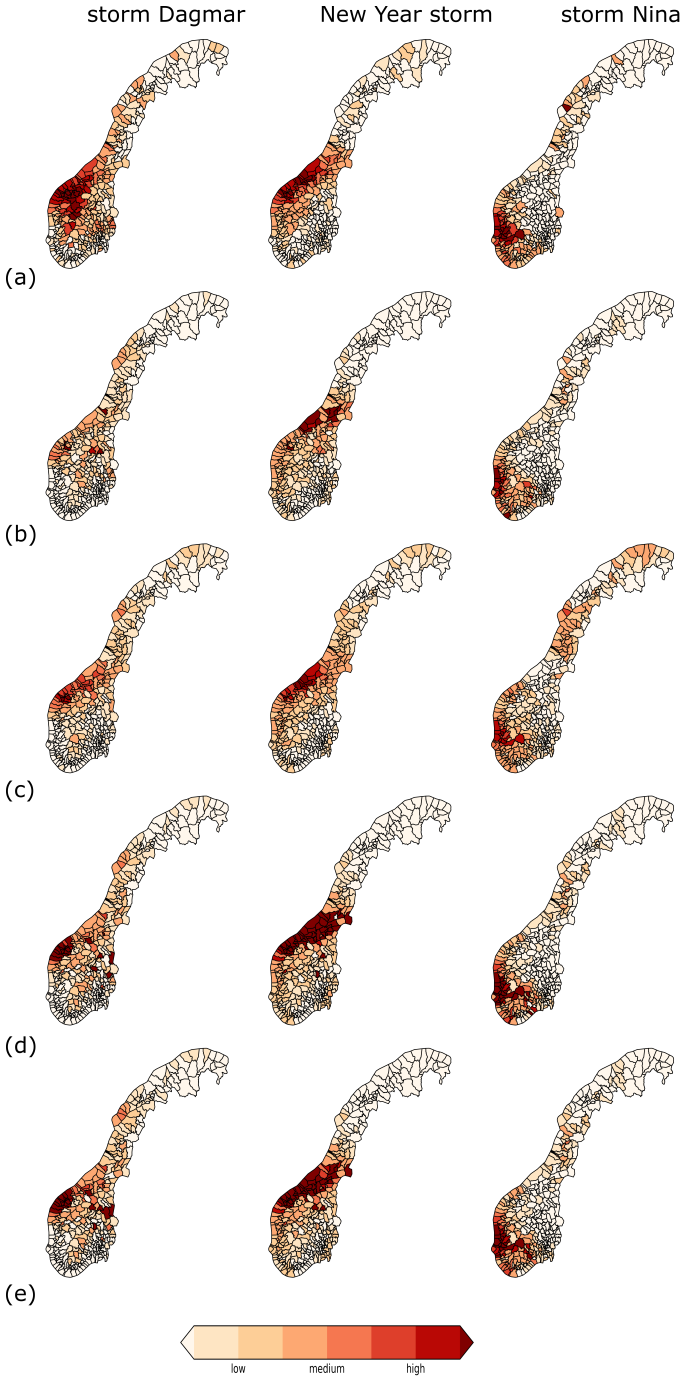


Figure S10: Spatial patterns of observed and estimated losses for the three most damaging events, where (a) display the observed losses and (b), (c), (d) and (e) are their estimates from the exponential, Klawa, modified Prahl and Prahl models respectively. The class boundaries of the colour bar are the 20th, 40th, 60th, 80th, 85th, 90th and 95th percentiles of the observed losses of their respective events. Table S2 shows the spatial correlations between observed and estimated losses.

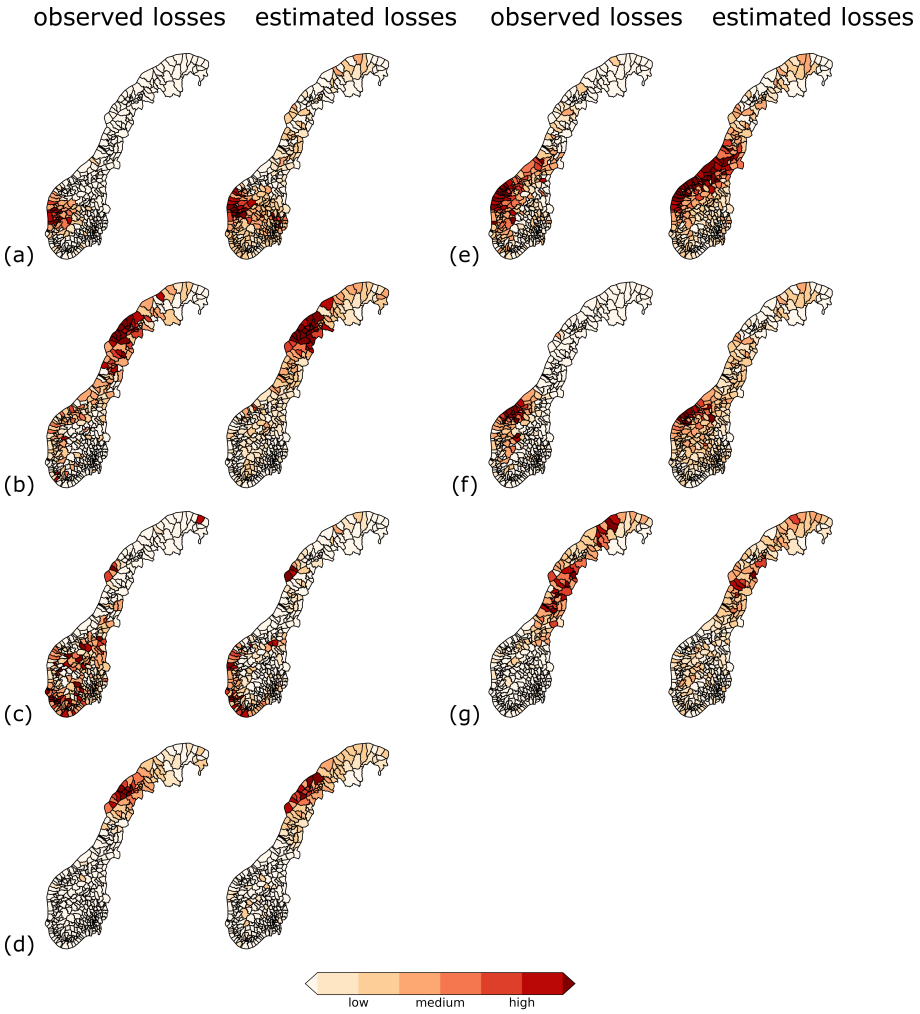


Figure S11: Spatial patterns of observed and estimated losses from the closest model to the observed loss for seven damaging events, where the panels represent (a) storm of 1994, (b) storm Ole, (c) storm of 1987, (d) storm Frode, (e) storm Tor, (f) storm of 1988 and (g) storm Narve. The Spearman rank correlation between observed and estimated losses of events are 0.46, 0.45, 0.44, 0.56, 0.51, 0.43 and 0.50 respectively. The class boundaries of the colour bar are the 20th, 40th, 60th, 80th, 85th, 90th and 95th percentiles of the observed losses of their respective events.

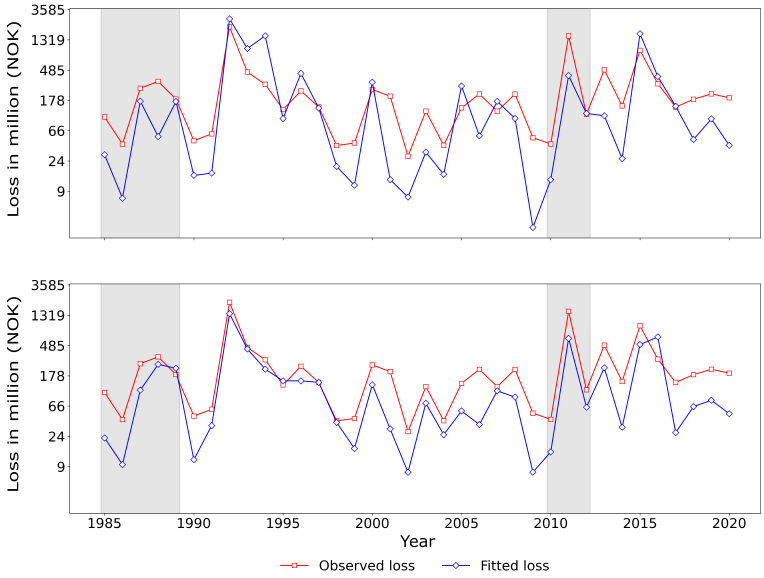


Figure S12: Annual time series of observed and estimated national losses for the extreme loss class from the deterministic exponential model (top) and deterministic model by Klawa (bottom). Note that the y-axis is logarithmic and the shaded region represents the testing period.

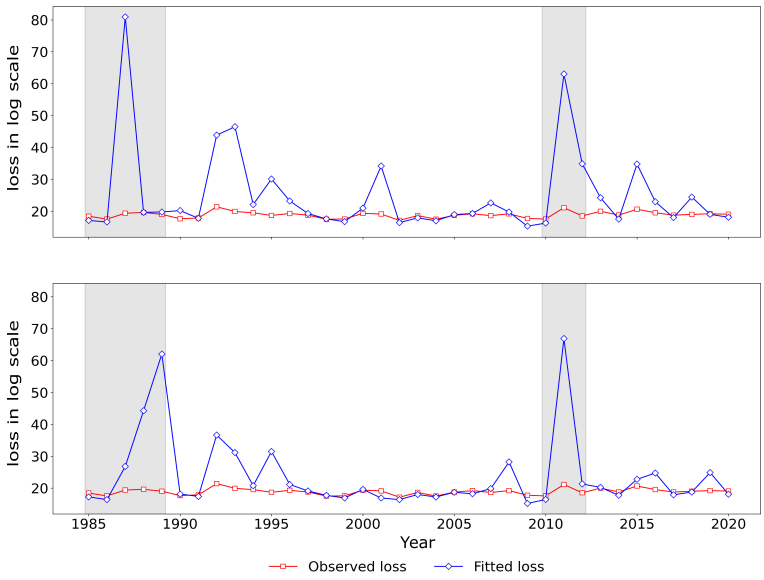


Figure S13: Same as Fig. S12 but using the probabilistic models: modified Prahl model (top) and model by Prahl (bottom). Note that the y-axis is logarithmic and the shaded region represents the testing period. Loss estimates from roughly 20% of the municipalities are responsible for the large margin between the observed and estimated losses.

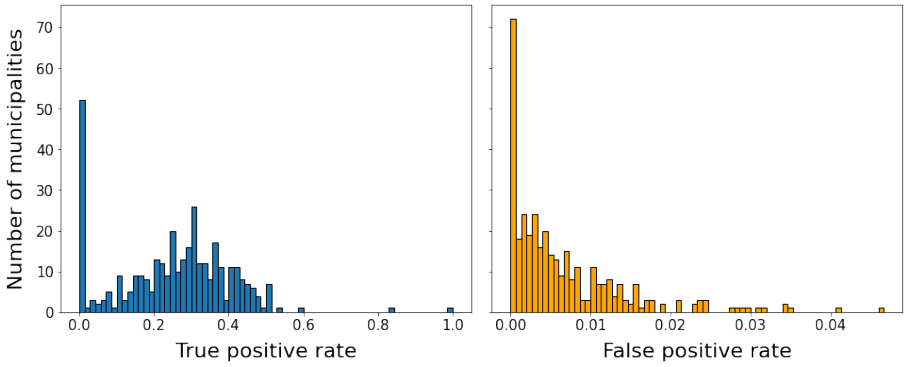


Figure S14: Distributions of the (left) true and (right) false positive rates of the damage classifier using the testing data.

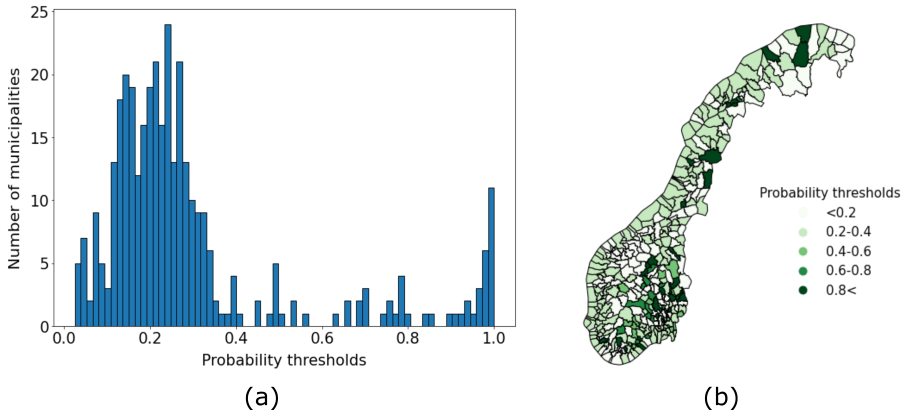


Figure S15: (a) Distribution of the probability thresholds for all municipalities and (b) map of the best probability thresholds for each municipality based on precision-recall curves and F-scores.

| Event | Number of claims | Loss in million NOK (2015) | Period | Region of impact |
|---|---|---|---|---|
| New Year storm | 22823 | 1933 | 01.01.1992 | Western Norway |
| Dagmar | 14247 | 1274 | 25.12.2011 - 27.12.2011 | Western Norway |
| Nina | 9525 | 593 | 09.01.2015 - 12.01.2015 | South-west Norway |
| Storm of 1994 | 5306 | 261 | 23.01.1994 | South-west Norway |
| Ole | 2418 | 237 | 07.02.2015 - 10.02.2015 | West and northern Norway |
| Storm of 1987 | 5014 | 235 | 16.10.1987 - 17.10.1987 | Southern Norway |
| Frode | 2876 | 234 | 12.10.1996 - 13.10.1996 | Northern Norway |
| Tor | 3940 | 214 | 29.01.2016 - 31.01.2016 | Western Norway |
| Storm of 1988 | 2853 | 184 | 22.12.1988 - 23.12.1988 | Central western Norway |
| Narve | 2080 | 182 | 17.01.2006 - 24.01.2006 | Northern Norway |

Table S1: Features of then most damaging storm events that occurred in Norway during the study period (1985-2020). The event periods are as defined by Norwegian Natural Perils Pool.

| Damage function | New year storm | storm Dagmar | storm Nina |
|---|---|---|---|
| Exponential | 0.57 | 0.64 | 0.66 |
| Klawa | 0.53 | 0.68 | 0.57 |
| Modified Prahl | 0.58 | 0.66 | 0.68 |
| Prahl | 0.58 | 0.67 | 0.67 |

Table S2: Spearman's rank correlation between observed and estimated losses of individual models for the three most damaging events.

| Event | Accuracy (%) | Recall (%) |
|---|---|---|
| New Year storm | 75.5 | 77 |
| Dagmar | 66.6 | 63.4 |
| Nina | 76.7 | 71.5 |
| Storm of 1994 | 69.7 | 86.7 |
| Ole | 69.7 | 60 |

Table S3: Classification accuracies and recall scores for the top five damaging wind events in Norway ordered with decreasing monetary loss (see Table S1). The accuracy column shows the proportion of municipalities in which the damage classifier accurately predicts both the events and non-events. Recall scores indicate the proportion of municipalities where the damage classifier was able to predict an event that actually occurred.

# References

Pinto, J. G., Fröhlich, E., Leckebusch, G., and Ulbrich, U.: Changing European storm loss potentials under modified climate conditions according to ensemble simulations of the ECHAM5/MPI-OM1 GCM, Natural Hazards and Earth System Sciences, 7, 165–175, https://doi.org/10.5194/nhess-7-165-2007, 2007.